

Electron-positron cascade in magnetospheres of supermassive Kerr black holes and the origin of relativistic AGN jets

MIKHAIL V. MEDVEDEV ^{1,2} AND ANDRZEJ A. ZDZIARSKI  ³

¹ Department of Physics and Astronomy, University of Kansas, Lawrence, KS 66045

² Laboratory for Nuclear Science, Massachusetts Institute of Technology, Cambridge, MA 02139

³ Nicolaus Copernicus Astronomical Center, Polish Academy of Sciences, Bartycka 18, PL-00-716 Warszawa, Poland

ABSTRACT

The avalanche mechanism of plasma production in active galactic nuclei (AGNs) is detailed, and constraints on system parameters needed for efficient electron-positron pair cascades are explored. Whether an AGN falls within this favorable parameter range may explain the observed radio-loud versus radio-quiet dichotomy. On the other hand, this study shows that cascades generate orders of magnitude fewer pairs than is necessary to explain the synchrotron emission observed in luminous jets. This fact suggests the existence of either an alternative lepton source, namely pair production of photons from the hot accretion flows around AGN central black holes, or matter loading of the jets from the surrounding medium, or, most likely, both. The case of the radio galaxy 3C 120 is considered in detail.

1. INTRODUCTION

Collimated relativistic jets are observed in a wide variety of astrophysical objects accreting plasmas with magnetic fields. Jets originating from systems containing black holes (BHs) are likely associated with accretion flows in them. These jet-producing BH systems span a wide range of parameters. For instance, BH masses span nearly ten orders of magnitude, from stellar-mass BHs in binaries and γ -ray bursts to supermassive BHs in radio-loud and radio-quiet galaxies, quasars, and active galactic nuclei (AGNs).

It is generally accepted that the physical mechanism responsible for the jet production is the collimation of the ejected plasma by magnetic fields. The physical mechanism identified to date for the launch of the most powerful jets is the Blandford-Znajek (BZ) mechanism, in which the rotational energy of a Kerr BH is tapped by large-scale magnetic fields threading the horizon (Blandford & Znajek 1977). This theoretical idea of the electromagnetic energy extraction of the BH rotation energy has been confirmed with numerical simulations (see, e.g., Semenov et al. 2004; Tchekhovskoy et al. 2011, 2012) and, possibly, in observations of stellar-mass BHs, through a claimed correlation between the radio luminosity of the transient ballistic jets and the BH spin parameters estimated via continuum fitting (Narayan & McClintock 2012; Steiner et al. 2013).

The BZ mechanism relies on the formation of an e^\pm cascade in the BH magnetosphere. In it, some seed electrons are accelerated by the electric fields, and then upscatter soft photons emitted by the surrounding accretion flow to energies above the threshold for pair production. Particle-in-cell simulations of such pair cascades in Kerr BH environments have been performed (Parfrey et al. 2019; Crinquand et al. 2020; Yuan et al. 2025). They demonstrate the feasibility of the pair-cascade model for explaining jet sources. In fact, the formation of such a cascade is a necessary condition for the BZ jet formation. Without it, the vacuum magnetosphere yields null jet power (Wald 1974).

On the other hand, the rate of e^\pm pairs produced in the cascade is very limited. It is usually parametrized by the ratio of the charge density in the magnetosphere to the Goldreich-Julian (GJ) density, whose order of magnitude estimate is

$$\rho_{\text{GJ}} \sim \frac{\omega_{\text{BH}} B}{4\pi c}, \quad (1)$$

where B is the strength of the magnetic field, c is the speed of light, and ω_{BH} is the angular velocity of BH rotation [see Eqs. (6), (7) below for the exact definitions of ω_{BH} and ρ_{GJ}]. The density ratio, $\lambda \equiv \rho_e / \rho_{\text{GJ}}$, is called the pair

multiplicity, and, for magnetospheric cascades, it is limited to $\lambda \lesssim 10^3$ (Levinson & Rieger 2011; Nokhrina et al. 2015). The corresponding lepton flux can be compared with that inferred from radio observations of luminous AGN jets (Nokhrina et al. 2015). Those authors⁴ found large values, $\lambda \gtrsim 10^{10}$. The magnetospheric cascades alone can account for the observed properties of only very weak sources, such as M87 and Sgr A* (e.g., Levinson & Rieger 2011; Mościbrodzka et al. 2011). This shows the necessity of the presence of another mechanism of lepton loading, either in the form of normal plasma or e^\pm pairs⁵.

A process likely to occur is e^\pm pair production at the base of a Poynting-flux-dominated jet via collisions of energetic photons emitted by a hot accretion flow (Henri & Pelletier 1991; Beloborodov 1999a; Levinson & Rieger 2011; Mościbrodzka et al. 2011; Aharonian et al. 2017; Sikora et al. 2020; Zdziarski et al. 2022a). Depending on the power and spectral characteristics of the hot flow, this process can be substantially more efficient than the magnetospheric cascade. However, this does not rule out the presence of baryon loading from the jet's surroundings, e.g., O' Riordan et al. (2018). In the case of the radio galaxy 3C 120, Zdziarski et al. (2022a) calculated both the rate of pair production within the jet base (based on the hard-X-ray spectrum) and the rate of flow of the synchrotron-emitting leptons (based on the synchrotron spectrum of the core jet) and found them to be compatible with being the same. Similar calculations, showing that these two rates are comparable, were performed for the microquasars MAXI J1820+070 and Cyg X-1 (Zdziarski et al. 2022b; Zdziarski & Egron 2022). Thus, at least in those sources, there is no necessity for a substantial baryon loading from the point of view of accounting for the synchrotron emission. On the other hand, some baryon loading is required, at least in some cases, to account for the jet energetics, e.g., Pjanka et al. (2017).

In this work, we re-examine the process of magnetospheric cascades. We provide simple analytical estimates of the process's properties and derive conditions under which it operates. We compare our results with previous numerical calculations. For 3C 120, we confirm that the rate of this process is many orders of magnitude lower than that inferred from the synchrotron spectrum. We also consider whether the well-known dichotomy between radio-loud and radio-quiet AGNs (e.g., Sikora et al. 2007) can be related to the derived condition for cascade formation.

2. ELECTRON-POSITRON CASCADE IN KERR BH MAGNETOSPHERES

An energetic, often relativistic, plasma is present in extreme astrophysical environments, including spinning neutron stars, magnetars, and spinning BHs of various masses, which drive powerful relativistic jets. Unlike a neutron star, where charges can be pulled from the surface and populate its environment, a BH horizon cannot be a source of plasma. The plasma source must therefore be within the magnetosphere, namely the external magnetic field (since a BH cannot have its own B -field), with self-generated plasma flowing away or falling in through the outer and inner light cylinders.

In the e^\pm avalanche model of pair production that we discuss here, the region where plasma is generated is called the “*spark gap*” (or just the “*gap*”). Depending on whether plasma can be produced in the magnetosphere, a relativistic jetted outflow may be present or absent in the system. Astronomical observations show that both possibilities exist in nature.

We should note that vacuum breakdown cannot occur, especially around supermassive BHs, because the induced electric fields are too low: $E \lesssim B \sim 10^5$ G $\ll E_{\text{Schwinger}}$, where

$$E_{\text{Schwinger}} \equiv \frac{m_e^2 c^3}{e \hbar} \approx 4.4 \times 10^{13} \text{ G} \quad (2)$$

is the critical field strength for spontaneous vacuum pair production, e and m_e are the electron charge and mass, respectively, and $\hbar = h/2\pi$ is the Planck constant. Yet, the leptonic pair plasma avalanche can be produced via a cascade initiated by seed charges accelerated in the spark-gap region, which scatter off photons emitted by an accretion flow. The cascade is a threshold process that depends on several system parameters.

To proceed, we need to set up the magnetic field geometry. If the plasma is sufficiently dense, the magnetosphere adopts a force-free configuration. The magnetic field takes a split-monopole solution (Figure 1) of the Grad-Shafranov equation, with the current sheet in the equatorial plane (Lyutikov 2012; Nathanail & Contopoulos 2014). It is known that the force-free condition breaks down in the regions of a weak (vanishing) magnetic field, e.g., in the current sheet. It is not considered to be a big problem, however, because the solution, which becomes formally discontinuous, can be readily regularized by putting in finite plasma inertia, finite Larmor radius of particles, collisionality, etc.

⁴ Nokhrina et al. (2015) reported $\lambda \gtrsim 10^{12}$, but assumed that only 1 in 100 leptons undergo acceleration.

⁵ We note that this fact is often overlooked, with statements in literature that BZ jets are by default pair-dominated, and a detection of baryons indicates a different type of the jet (e.g., Díaz Trigo et al. 2013).

For the force-free condition to hold, the amount of plasma should be enough to short-circuit the electric field component along the magnetic field (particle drifts of charges perpendicular to the B -field are slow and can be neglected). BHs have inner and outer light cylinders — the imaginary surfaces through which the plasma can move away from the stagnation surface inward or outward, respectively, as is shown in Figure 1. These plasma flows should evacuate the entire region between them, unless the plasma is replenished. If the plasma is not replenished in the required quantities, the magnetosphere is *not* force-free. Instead, it is represented by the vacuum solution (Wald 1974), which yields vanishing BZ jet power. In other words, the jet is nonexistent in a vacuum field configuration when the plasma replenishment process ceases.

2.1. The cascade model

Let us first assume that there is initially no plasma in a small region, called the spark gap region, of the BH magnetosphere near the null surface, where the GJ charge density vanishes, $\rho_{GJ} = 0$. Because this region is small, the absence of plasma does not violate the global force-free structure of the magnetosphere, although the force-free approximation is generally invalid locally. Furthermore, if the gap size is small compared to its radial distance, $H \ll R$, the deviation from the force-free B -field geometry within the gap is negligible, too. Since the plasma is absent in the gap region, an uncompensated electric field can exist along the magnetospheric magnetic field. This electric field can accelerate charges to large energies, which can subsequently be converted into electron-positron pairs via the avalanche mechanism. Thus, the gap region is the natural site for abundant plasma production.

The avalanche mechanism goes as follows. (i) A non-compensated parallel electric field accelerates a seed charge in the spark gap region. Provided the electric field and the gap size are large enough, the charge is accelerated to a relativistic energy, so its Lorentz factor is $\Gamma \gg 1$. (ii) The charge is propagating in the magnetosphere in a “bath” of soft photons copiously produced by the accretion disk. Incidentally, the charge can Compton up-scatter a soft background photon to a hard γ -ray photon, $e + \gamma_b \rightarrow e + \gamma_\gamma$. (iii) Finally, a γ -ray photon interacting with a soft photon can produce an electron-positron pair, $\gamma_\gamma + \gamma_b \rightarrow e^+ + e^-$, provided that their total center-of-mass energy exceeds the electron rest energy, $m_e c^2$. These secondary charges are accelerated by the parallel electric field, producing more γ -rays and more charges exponentially.

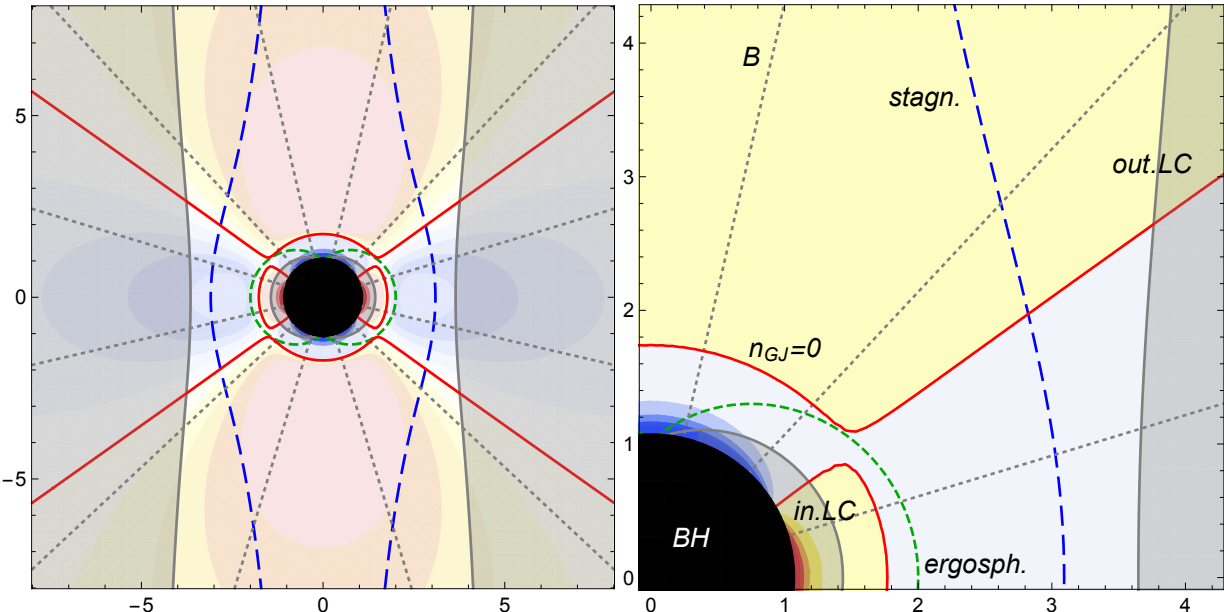


Figure 1. Schematic representation of the accreting BH system. Shown are the ergosphere (green dashed curves), inner and outer light cylinders (gray lines and shades), magnetic field lines (dotted lines), stagnation surface (blue dashed curves), and the GJ null surface (red curves). Yellow-orange and blue indicate positive and negative charge densities, respectively. An accretion disk (not shown) is in the equatorial plane. We assume a rapidly spinning BH with $a_* = 0.99$ and $\omega_F = 0.45\omega_{BH}$. Axes scales are in units of r_g .

2.1.1. Electric field and Lorentz factor

Assuming a stationary axisymmetric degenerate force-free magnetosphere around a rotating BH, the electric field is only in the poloidal direction (Hirotani & Okamoto 1998):

$$E_p = -\frac{\omega_F - \omega}{2\pi\alpha c} \nabla \Psi, \quad (3)$$

where Ψ is the magnetic flux and ω_F is the angular velocity of the magnetic field lines, α is the redshift factor (also referred to as the lapse function), and ω is the angular velocity of the zero angular momentum observer (ZAMO), which keeps their r and θ coordinates constant. These parameters are defined in Kerr geometry, conventionally written in Boyer–Lindquist coordinates as

$$\alpha = \rho \Delta^{1/2} / \Sigma, \quad (4)$$

$$\omega = 2a r_g c / \Sigma^2, \quad (5)$$

where $r_g = GM/c^2$ is the radius of the extremely spinning Kerr black hole, $\rho^2 = r^2 + a^2 \cos^2(\theta)$, $\Delta = r^2 - 2r_g r + a^2$, $\Sigma^2 = (r^2 + a^2)^2 - a^2 \Delta \sin^2(\theta)$, and $a = J/Mc$ is the spin parameter (Thorne et al. 1986; Beskin et al. 1992; Hirotani & Okamoto 1998). Note that often, one conveniently uses the dimensionless spin parameter defined as $a_* = Jc/(GM^2) = a/r_g$ with $0 \leq a_* \leq 1$. Furthermore, the radius of an arbitrarily spinning BH is defined as the outer-horizon radius $r_{\text{BH}}(a_*) = r_g(1 + \sqrt{1 - a_*^2})$. We also note that the ZAMO angular velocity, ω , vanishes at infinity, $\alpha \rightarrow 1$, and coincides with the uniform rotation of the BH with angular velocity (Misner et al. 1973; Blandford & Znajek 1977)

$$\omega_{\text{BH}} \equiv \frac{a_* c}{2r_{\text{BH}}} = \frac{c}{2r_g} \left(\frac{a_*}{1 + \sqrt{1 - a_*^2}} \right) \quad (6)$$

as one approaches the horizon, $\alpha \rightarrow 0$. The local GJ charge density is:

$$\rho_{\text{GJ}} = \frac{1}{4\pi} \nabla \cdot E_p = -\frac{1}{4\pi} \nabla \cdot \left(\frac{\omega_F - \omega}{2\pi\alpha c} \nabla \Psi \right). \quad (7)$$

E_p changes sign when $\omega_F = \omega$; therefore, ρ_{GJ} also changes sign. Consequently, there is a surface where ρ_{GJ} vanishes and is charge-deficient, leading to the emergence of an electric field along the magnetic field lines, E_{\parallel} , which breaks the force-free condition. This leads to the formation of a gap region (similar to the outer gap around a pulsar). We should note that ω_F is not generally known from the first principles. For analytical estimates, one often chooses that $\omega_F = 0.5\omega_{\text{BH}}$, which maximizes the BZ power. Numerical simulations indicate that the jet power, and hence ω_F , varies across different accretion systems (e.g., (Lowell et al. 2024)).

Poisson's equation inside the gap is:

$$dE_{\parallel}/dx = 4\pi[e(n^+ - n^-) - \rho_{\text{GJ}}], \quad (8)$$

where n^{\pm} is the number density of positrons and electrons, respectively, generated and moving in the gap. Assuming the gap is thin, one uses a 1D representation of the gap, with $x = 0$ being in the middle of the gap, where $\rho_{\text{GJ}} = 0$, and having \hat{x} perpendicular to the null surface. Thus, r_0 is the radial position where $\rho_{\text{GJ}} = 0$ and the x -coordinate is $x = r - r_0$. Since the split-monopole field geometry is assumed, x is also the coordinate along a field line (where the charges are moving along it).

The total width of the gap, H , where the parallel electric field is non-vanishing, is small compared to the size of the extremely spinning Kerr BH, $r_g \approx 1.5 \times 10^{13} \text{ cm } M/10^8 M_{\odot}$, so one can expand $\rho_{\text{GJ}}(x)$ around $x = 0$. This expansion yields $\rho_{\text{GJ}}(x) \simeq Ax$, where $A = \partial_x(\rho_{\text{GJ}})$ at $x = 0$. In general, the parameter A is some complicated function of the BH mass and spin parameter, M and $0 \leq a \leq r_g$, and the azimuthal angle θ for a given distribution of the magnetospheric magnetic field near the horizon. From Poisson's equation, Equation (7), we have $E_{\parallel} = 4\pi A(x^2/2 - H^2/8)$ inside the gap, $0 \leq |x| \leq H/2$, and $E_{\parallel} = 0$ at $x = \pm H/2$ and beyond.

The electric field in the gap accelerates the charges. The motion of the charges as they are accelerated along the magnetic field lines can be approximated one-dimensionally (Hirotani & Okamoto 1998):

$$m_e c^2 d\Gamma/dx = eE_{\parallel} - \frac{4}{3}(\Gamma^2 - 1)\sigma_T U_b, \quad (9)$$

where σ_T is the Thomson cross section, Γ is the electron Lorentz factor, and U_b is the energy density of the background photons. The first term on the right-hand side is the acceleration due to the gap-parallel electric field, and the second is the Compton drag from the background photons. In this context, we disregard curvature radiation, as it is negligible given the substantial curvature radius, which is comparable to or larger than the size of supermassive BHs.

2.1.2. Inverse Compton scattering and pair production

Under the assumptions that all motion is along the electric field lines and the e^\pm spectrum is monoenergetic at a given position, the continuity equations of e^\pm s are

$$\pm d_x [n^\pm(x)\beta(x)] = \int_0^\infty \eta_p(\nu_\gamma)[F^+(x, \nu_\gamma) + F^-(x, \nu_\gamma)]d\nu_\gamma , \quad (10)$$

where $\beta(x)c$ is the electron velocity, F^\pm are the number densities of γ -rays propagating in the $\pm x$ -direction. The pair-production redistribution function, η_p , is the spectrum-averaged and angle-averaged cross-section; it is discussed in detail in [Hirotani & Okamoto \(1998\)](#), [Berestetskii et al. \(1982\)](#). Using Equation (10), one can see that the current in the gap along a field line is conserved along x , which yields an expression for the current density, $e[n^+(x) + n^-(x)]c\beta(x) = j_0$.

The γ -ray fluxes $F^\pm(x, \nu_\gamma)$ for each γ -ray photon energy, $h\nu_\gamma$ are described by the continuity equation:

$$\pm \partial_x F^\pm(x, \nu_\gamma) = \eta_C n^\pm \beta(x) - \eta_p F^\pm(x, \nu_\gamma) , \quad (11)$$

where η_C is the Compton redistribution function (i.e., the spectrum-averaged cross-section) and is discussed in detail in [Beskin et al. \(1992\)](#) and [Hirotani & Okamoto \(1998\)](#). For the behavior of the charges and γ -rays in the gap to be fully described, we need to choose a spectrum for the background photons.

The system of Equations (8), (9), (10), (11) supplied with appropriate boundary conditions can be solved numerically. The results are reported in detail elsewhere ([Ford et al. 2018](#); [Sitarz et al. 2024](#)). Their relevant aspects will be discussed where relevant.

2.2. Estimates

Now, we present estimates that help us to better understand the pair cascade and draw important conclusions.

2.2.1. Electric field

We can write the field strength as follows

$$E_\parallel \sim AH^2 \sim a_* B (H/r_g)^2 , \quad (12)$$

where we used the heuristic estimate for the GJ density $\rho_{GJ} \sim a_* B/r_g$, cf. Equation (1). It has the correct asymptotic values for both a non-spinning BH, $\rho_{GJ} = 0$ for $a_* = 0$, and a rapidly spinning BH, $\rho_{GJ} \sim B/r_g$ for $a_* \sim 1$ (i.e., for $a \sim GM/c^2$). Physically, this electric field is the motional field caused by general relativistic frame dragging measured in the rotating plasma frame. Thus, we can write

$$E_\parallel \simeq \beta_F B , \quad (13)$$

where $\beta_F \simeq v_F/c$ is of the order of the velocity of the field lines frozen in the ambient rotating plasma relative to the ZAMO frame. Note that $\beta_F \sim a_* (H/r_g)^2$, cf. Equations (12), (13).

2.2.2. Lepton acceleration

The number of soft photons is usually sufficiently large to produce a strong drag force, so a charge accelerated within the gap quickly attains a terminal relativistic velocity ([Hirotani & Okamoto 1998](#)). It is obtained from Equation (9) by setting $d\Gamma/dx = 0$ and $\Gamma \gg 1$. The terminal Lorentz factor is

$$\Gamma^2 \simeq \frac{eE_\parallel}{\sigma_T U_b} . \quad (14)$$

This expression is based on two assumptions, namely that (i) the Compton drag length, ℓ_C , is smaller than the pair-production length, ℓ_\pm , and (ii) both are smaller than the gap size, H , that is $\ell_C \ll \ell_\pm \ll H$. For the typical

conditions used in our paper, these are $\ell_C \sim 10^8$ cm, $\ell_{\pm} \sim 10^{10}$ cm, and $H \sim 10^{12}$ cm (Hirotani & Okamoto 1998) for a supermassive BH of mass $M \sim 10^8 M_{\odot}$, with H being about 7% of r_g .

In what follows, it is convenient to introduce the energy density in background photons corresponding to the Eddington luminosity:

$$U_{\text{Edd}} = \frac{L_{\text{Edd}}/c}{4\pi r_d^2} = \frac{4\pi GMm_p}{\sigma_T(4\pi r_d^2)}, \quad (15)$$

where m_p is the proton mass and $L_{\text{Edd}} \simeq 1.25 \times 10^{46} (M/10^8 M_{\odot})$ erg/s is the Eddington luminosity. It is assumed here that the Eddington luminosity of the BH+disk system is defined at approximately the half-power radius of the accretion disk, which, in turn, depends on the spin of the BH (Page & Thorne 1974; Fabian et al. 2014) as

$$r_d \simeq [5 + 28(1 - a_*)]r_g \equiv f_d r_g. \quad (16)$$

The “disk factor,” f_d , ranges between $f_d \sim 5$ for rapidly spinning BHs and $f_d \sim 33$ for slowly spinning BHs. Furthermore, the region above the disk is optically thin, so not all photons emitted from the disk (presumably isotropically) can reach the gap. Thus, the energy density of the soft disk photons entering the gap is smaller by the factor $\Omega_d/4\pi$, where Ω_d is the solid angle of the disk as seen from the gap location. Now, we normalize the energy density in the soft photons to this Eddington value:

$$U_b = \epsilon_b U_{\text{Edd}} \simeq \frac{\epsilon_b}{f_d^2} \frac{m_p c^2}{\sigma_T r_g} \sim (3 \times 10^4 \text{ erg cm}^{-3}) \epsilon_{b,-2} f_{d,1}^{-2} M_8^{-1}, \quad (17)$$

where $M_8 = M/(10^8 M_{\odot})$, $f_{d,1} = f_d/10^1$, $\epsilon_{b,-2} = \epsilon_b/10^{-2}$, and $\epsilon_b = (\Omega_d/4\pi)(L_b/L_{\text{Edd}})$ is the luminosity of the background radiation field in the gap region normalized to the Eddington luminosity. It is important to note that the factor ϵ_b is not just the standard “Eddington ratio” but also incorporates the disk solid angle factor $\Omega_d/4\pi$.

Finally, substituting E_{\parallel} and U_b in Equation (14), we have

$$\Gamma^2 \simeq (eB/m_p c)(r_g/c)\beta_F \epsilon_b^{-1} f_d^2 \sim 5 \times 10^{15} \beta_F \epsilon_{b,-2} f_{d,1}^2 M_8 B_5, \quad (18)$$

where $B_5 = B/(10^5 \text{ G})$.

2.2.3. Cascade threshold 1: energy

The formation of an avalanche is a threshold process driven by two independent “reactions”. First, inverse Compton scattering produces a γ -ray photon, $e + \gamma_b \rightarrow e + \gamma_{\gamma}$. Second, this gamma photon interacts with a background one to produce an electron positron pair, $\gamma_{\gamma} + \gamma_b \rightarrow e^+ + e^-$ (interactions of two γ -ray photons occur too, but they are rare, hence omitted). The latter is possible only if the energy of the γ -ray photon is enough for pair production. In the center of momentum frame, this energy condition is written as

$$\sqrt{h\nu_{\gamma} h\nu_b} \geq m_e c^2. \quad (19)$$

Here, we assumed a head-on collision, which yields the minimum energy requirement. In turn, inverse Compton scattering increases the soft photon energy by a factor of Γ^2 , i.e., $h\nu_{\gamma} \sim \Gamma^2 h\nu_b$.

Thus, the ‘energy threshold’ constraint on the soft photon energy reads:

$$h\nu_b \geq m_e c^2 / \Gamma. \quad (20)$$

2.2.4. Cascade threshold 2: multiplicity

The above processes should be efficient enough that the number of produced secondaries exceeds that of the initial primary leptons. In other words, the number of produced leptons per one primary lepton should exceed unity, i.e., the multiplicity should be greater than one. Otherwise, an exponential increase in the number of charges in the gap does not occur, so no avalanche can form.

The production rates (per length) of the gamma photons and the leptons are

$$dN_{\gamma}/dx \sim \sigma_T N_b N_{\pm}, \quad (21)$$

$$dN_{\pm}/dx \sim 2\sigma_{\pm} N_b N_{\gamma}. \quad (22)$$

where σ_{\pm} is the pair photo-production cross-section and N_b , N_{γ} , N_{\pm} are the particle densities of the soft photons, hard photons, and leptons, respectively. They can be combined to yield the lepton-production equation:

$$d^2N_{\pm}/dx^2 \sim 2\sigma_T\sigma_{\pm}N_b^2N_{\pm}. \quad (23)$$

The multiplicity of pair production inside the entire gap should exceed unity:

$$2\sigma_T\sigma_{\pm}N_b^2H^2 > 1. \quad (24)$$

This is the ‘multiplicity threshold’.

We note that Equations (21) and (22) are simplified versions of Equations (11) and (10), respectively, where the functions η_C and η_p involve cross-sections σ_T , σ_{\pm} . It is worthwhile to emphasize that the γ -ray photon fluxes are essentially counter-propagating. Indeed, the high-energy γ -ray photons are produced via Compton scattering by highly-relativistic, counter-propagating electrons and positrons accelerated by the same electric field along the background B -field.

For our order-of-magnitude estimates here, we assume that (i) background photons are mono-energetic, (ii) the Compton scattering cross-section is simply the Thompson cross-section (i.e., neglecting Klein-Nishina corrections), and (iii) the pair production cross-section averaged over an isotropic distribution of seed photons is approximately (Gould & Schréder 1967; see Brown et al. 1973 for corrections)

$$\langle\sigma_{\pm}\rangle \approx \frac{3}{4}\frac{\sigma_T}{\Gamma_{\gamma b}^2} (\ln 4\Gamma_{\gamma b}^2 - 2) \simeq \frac{\sigma_T}{\Gamma_{\gamma b}^2} \ln \Gamma_{\gamma b}, \quad (25)$$

where $\Gamma_{\gamma b} \equiv \sqrt{h\nu_{\gamma}h\nu_b}/m_e c^2 \simeq \Gamma h\nu_b/m_e c^2$ and $\Gamma_{\gamma b} \gg 1$ was assumed. For a mono-energetic background, $N_b \sim U_b/h\nu_b$. The ‘multiplicity threshold’ now reads:

$$(h\nu_b)^2 \leq \sqrt{2 \ln \Gamma_{\gamma b}} (\sigma_T/\Gamma)(m_e c^2) U_b H. \quad (26)$$

For practical cases, the factor $\sqrt{2 \ln \Gamma_{\gamma b}}$ is of the order of a few. It is omitted from our further estimates for simplicity.

2.3. Results

We now combine the two avalanche threshold conditions given by Equations (20), (26):

$$\frac{1}{\Gamma} \leq \frac{h\nu_b}{m_e c^2} \leq \left(\frac{\epsilon_b}{\Gamma f_d^2} \frac{m_p}{m_e} \frac{H}{r_g} \right)^{1/2}. \quad (27)$$

Now, using Equation (18) and recalling that $\beta_F \sim (H/r_g)^2$, one obtains:

$$2 \times 10^{-6} \left(\frac{\epsilon_{b,-2}}{a_* f_{d,1}^2 M_8 B_5 h_{g,-2}^2} \right)^{1/2} \lesssim \frac{h\nu_b}{m_e c^2} \lesssim 6 \times 10^{-5} \left(\frac{\epsilon_{b,-2}^3}{a_* f_{d,1}^6 M_8 B_5} \right)^{1/4} \quad (28)$$

where $h_g = H/r_g$ is the dimensionless gap size, $h_{g,-2} = h_g/10^{-2}$, and we remind that the normalized disk factor is BH-spin-dependent, $f_{d,1} \simeq 0.5 + 2.8(1 - a_*)$.

This is an interesting and useful result. Indeed, Equation (28) shows that only soft photons within a fairly narrow optical-to-UV range can produce a leptonic avalanche. In this case, we can expect a strong AGN jet. If the conditions are not right, e.g., the magnetic field is too low, or the background spectral distribution is not optimal (ϵ_b is too low), the cascade cannot form. For example, the fields below $B \sim 1$ G should completely suppress the cascade process. In this case, no plasma is produced; hence, no BZ-powered jet is present. One can argue that this mechanism can explain the observed radio-loud/radio-quiet galaxy dichotomy.

The above calculations are useful estimates but cannot replace actual numerical modeling. The numerical results and the instructive scalings of the system parameters are reported elsewhere (Ford et al. 2018; Sitarz et al. 2024).

Furthermore, a recent study of 3C 120 (Zdziarski et al. 2022a) quantitatively confirms (and extends) previous work, suggesting that an alternative mechanism is responsible for jet production in luminous sources. This is discussed in the next section.

3. AN EXAMPLE OF 3C 120

3C 120 is a nearby radio galaxy at a redshift of 0.033. Its mass is $M \approx (7 \pm 2) \times 10^7 M_\odot$ (Grier et al. 2017), and its accretion luminosity was estimated as $L_{\text{accr}} \approx 1 \times 10^{45} \text{ erg s}^{-1}$ (Janiak et al. 2016), which corresponds to an Eddington ratio of ~ 0.1 . It features a powerful jet (Marscher et al. 2002), observed at radio, infrared, and high-energy γ -ray wavelengths. However, its X-ray emission is dominated by a hot accretion flow, as evidenced by its spectrum, which includes both a power-law component characteristic of Comptonization and strong X-ray Compton reflection features (Zdziarski & Grandi 2001; Lohfink et al. 2013). This accretion flow emission was also detected in soft γ -rays (Woźniak et al. 1998). This rare combination of observational features allows the pair-production rate at the base of the jet (Beloborodov 1999b; Levinson & Rieger 2011) to be estimated from the spectrum of photons emitted by the hot accretion flow. At the same time, the synchrotron spectrum emitted by its core jet (Giommi et al. 2012) allows estimating the flow rate of the relativistic leptons responsible for that emission.

These quantities were estimated by Zdziarski et al. (2022a) as $2\dot{N}_+ \approx 3.9_{-2.8}^{+6.3} \times 10^{49} \text{ s}^{-1}$ and $\dot{N}_e \approx 2.7_{-2.3}^{+12} \times 10^{49} \text{ s}^{-1}$, respectively. Within the uncertainties, they are compatible with being the same, showing that the rate of pair production by photons from the hot accretion is fully capable of accounting for the flow of synchrotron-emitting leptons far in the jet. Furthermore, the theoretically achievable jet power (Davis & Tchekhovskoy 2020 and references therein) corresponds to a BZ jet launched from a magnetically arrested flow and is given by $P_j \lesssim a_*^2 M_{\text{accr}} c^2 = a_*^2 L_{\text{accr}} / \epsilon$, where $\epsilon \sim 0.1$ is the accretion efficiency. This limits the jet power to $P_j \lesssim 1 a_*^2 \times 10^{46} \text{ erg s}^{-1}$. If the synchrotron-emitting leptons were mostly electrons, the jet power in the associated ions would be (Zdziarski et al. 2022a) $P_j \approx 3.1_{-2.8}^{+19.6} \times 10^{47} (\epsilon/0.1)^{-1} \text{ erg s}^{-1}$, violating the theoretical constraint on the jet power by at least of factor of 10. This, in turn, implies that abundant e^\pm pairs are present in the jet of 3C 120 and dominate (by number, but not by weight) its composition. This also agrees with the general estimates of Sikora et al. (2020).

We can also estimate the strength of the poloidal magnetic field that threads the BH on one hemisphere. The power of a BZ jet can also be written as $P_j \approx (\phi/50)^2 a_*^2 M_{\text{accr}} c^2$, where $\phi \lesssim 50$ (e.g., Davis & Tchekhovskoy 2020) is a dimensionless magnetic flux defined by $\phi \equiv 2\pi B r_g / (M_{\text{accr}} c)^{1/2}$. Given that $P_j \lesssim a_*^2 L_{\text{accr}} / \epsilon$ (see above), we obtain $B \lesssim 4 \times 10^5 \text{ G}$, where the maximum corresponds to magnetically arrested accretion.

3.1. Comparison with the avalanche model

The observational data indicate that the avalanche conditions in Equation (28) are satisfied in 3C 120. However, is the theoretical pair-production rate in magnetospheric cascades sufficient to account for the data?

The minimum estimate is based on the GJ density. Indeed, n_{GJ} is the minimum plasma density needed to short-circuit the parallel electric field in the rotating magnetosphere (except for a small gap region). This is also the boundary condition stating that $E_{\parallel} = 0$ at $|x| = \pm H/2$, in the numerical model. In fact, this condition self-consistently determines the gap size, H . On the other hand, this plasma is relativistic and evacuates the magnetosphere with $v \sim c$. The corresponding particle flux density is simply $n_{\text{GJ}} c$.

The GJ density is obtained from Poisson's equation, Equation (7), with $E_p \sim a_* B$. Thus,

$$n_{\text{GJ}} \sim a_* B / (4\pi e r_g) \sim (1 \text{ cm}^{-3}) a_* M_8^{-1} B_5. \quad (29)$$

This is consistent with the numerical studies by Ford et al. (2018); Sitarz et al. (2024). The corresponding GJ-based *lower limit* on the lepton production rate, which is equal to the total particle flux, is

$$\dot{N}_{\text{min}} \sim n_{\text{GJ}} c (4\pi r_g^2) \sim (9 \times 10^{37} \text{ s}^{-1}) a_* M_8 B_5. \quad (30)$$

For the case of 3C 120 with $M \sim 7 \times 10^7 M_\odot$ and $B \sim 4 \times 10^5 \text{ G}$, we get $\dot{N}_{\text{min}} \sim 3 \times 10^{38} \text{ s}^{-1}$ at $a_* \approx 1$. This is many orders of magnitude lower than the observed rate of lepton flow through the jet of $\dot{N}_e \sim 10^{49} \text{ s}^{-1}$.

We note that the actual pair-production rate may be substantially higher because many γ -ray photons produced in the gap region propagate farther and continue to produce pairs far from the gap (Levinson & Rieger 2011). The *upper limit* on pair production is obtained by assuming that all the energy contained in γ -ray photons is ultimately converted into e^\pm pairs. To do this, we use the scaling relation for the total γ -ray luminosity of the cascades obtained from the self-consistent numerical solution, Equation (40) in Ford et al. (2018), which we quote here:

$$\frac{dL_\gamma}{d\Omega} \simeq (2.5 \times 10^{35} \text{ erg s}^{-1} \text{ sr}^{-1}) a_*^{0.96} \left(\frac{M}{10^7 M_\odot} \right)^{-2.5} \left(\frac{B}{10^4 \text{ G}} \right)^{0.95} \left(\frac{U_b}{10^6 \text{ erg/cm}^3} \right)^{1.17}. \quad (31)$$

The maximum pair production rate then becomes

$$\dot{N}_{\max} \sim (3 \times 10^{40} \text{ s}^{-1}) a_* M_8^{-2.5} B_5 \epsilon_b^{1.2} f_{d,1}^{-2.4}, \quad (32)$$

where we rounded up the exponents. For 3C 120, this yields $\dot{N}_{\max} \sim 4 \times 10^{41} \text{ s}^{-1}$ even for a maximally spinning BH, $a_* = 1$ and $f_d = 5$, accreting at the Eddington limit and having a huge disk solid angle $\Omega_d = 4\pi$, so that $\epsilon_b = 1$. This rate still remains much too low to account for the observations.

4. CONCLUSIONS

We have explored the cascade mechanism for the production of e^\pm pairs in an AGN environment. Such cascades are necessary for jet formation via the BZ mechanism. We have obtained crucial constraints on the magnetic field strength and the seed-photon field under which the leptonic cascade is possible. Whether these constraints are satisfied or not may explain the radio-loud/radio-quiet dichotomy.

On the other hand, we find that the rate of production of e^\pm pairs in the cascade mechanism is very limited. They alone may account for the rate of particles flowing through the jet only for very weak sources, possibly M87 or Sgr A*. In luminous sources, such as bright radio galaxies or blazars, the rate of the lepton flow as inferred from the jet synchrotron emission can be orders of magnitude higher than the maximum rate achievable in magnetospheric cascades. We detail this issue for the case of the bright radio galaxy 3C 120. In that case, the cascade rate is limited to less than 4×10^{41} particles per second. This rate is several orders of magnitude lower than the value deduced from the synchrotron emission of its core jet of about 10^{49} particles per second.

Thus, another mechanism for plasma production must be at work in luminous jet sources. Such a process is most likely the direct pair creation in the hot accretion disk's photon field, as suggested in several previous works. This has been quantitatively confirmed in the case of 3C 120, where the synchrotron-inferred lepton flow rate was found to be compatible (within the model and observational uncertainties) with the pair production rate inferred from its X-ray and soft γ -ray spectrum.

ACKNOWLEDGEMENTS

MVM acknowledges support by the National Science Foundation via grant NSF PHY-2409249 and partial support via grant NSF PHY-2309135 to the Kavli Institute for Theoretical Physics (KITP). AAZ acknowledges support from the Polish National Science Center grants 2019/35/B/ST9/03944 and 2023/48/Q/ST9/00138.

REFERENCES

Aharonian, F. A., Barkov, M. V., & Khangulyan, D. 2017, *ApJ*, 841, 61, doi: [10.3847/1538-4357/aa7049](https://doi.org/10.3847/1538-4357/aa7049)

Beloborodov, A. M. 1999a, *MNRAS*, 305, 181, doi: [10.1046/j.1365-8711.1999.02384.x](https://doi.org/10.1046/j.1365-8711.1999.02384.x)

—. 1999b, *ApJL*, 510, L123, doi: [10.1086/311810](https://doi.org/10.1086/311810)

Berestetskii, V. B., Lifshitz, E. M., & Pitaevskii, V. B. 1982, *Quantum electrodynamics* (Oxford: Pergamon Press)

Beskin, V. S., Istomin, Y. N., & Par'ev, V. I. 1992, *AZh*, 69, 1258

Blandford, R. D., & Znajek, R. L. 1977, *MNRAS*, 179, 433, doi: [10.1093/mnras/179.3.433](https://doi.org/10.1093/mnras/179.3.433)

Brown, R. W., Mikaelian, K. O., & Gould, R. J. 1973, *Astrophys. Lett.*, 14, 203

Criniquand, B., Cerutti, B., Philippov, A., Parfrey, K., & Dubus, G. 2020, *PhRvL*, 124, 145101, doi: [10.1103/PhysRevLett.124.145101](https://doi.org/10.1103/PhysRevLett.124.145101)

Davis, S. W., & Tchekhovskoy, A. 2020, *ARA&A*, 58, 407, doi: [10.1146/annurev-astro-081817-051905](https://doi.org/10.1146/annurev-astro-081817-051905)

Díaz Trigo, M., Miller-Jones, J. C. A., Migliari, S., Broderick, J. W., & Tzioumis, T. 2013, *Nature*, 504, 260, doi: [10.1038/nature12672](https://doi.org/10.1038/nature12672)

Fabian, A. C., Parker, M. L., Wilkins, D. R., et al. 2014, *MNRAS*, 439, 2307, doi: [10.1093/mnras/stu045](https://doi.org/10.1093/mnras/stu045)

Ford, A. L., Keenan, B. D., & Medvedev, M. V. 2018, *PhRvD*, 98, 063016, doi: [10.1103/PhysRevD.98.063016](https://doi.org/10.1103/PhysRevD.98.063016)

Giommi, P., Polenta, G., Lähteenmäki, A., et al. 2012, *A&A*, 541, A160, doi: [10.1051/0004-6361/201117825](https://doi.org/10.1051/0004-6361/201117825)

Gould, R. J., & Schréder, G. P. 1967, *Physical Review*, 155, 1404, doi: [10.1103/PhysRev.155.1404](https://doi.org/10.1103/PhysRev.155.1404)

Grier, C. J., Pancoast, A., Barth, A. J., et al. 2017, *ApJ*, 849, 146, doi: [10.3847/1538-4357/aa901b](https://doi.org/10.3847/1538-4357/aa901b)

Henri, G., & Pelletier, G. 1991, *ApJL*, 383, L7, doi: [10.1086/186228](https://doi.org/10.1086/186228)

Hirotani, K., & Okamoto, I. 1998, *ApJ*, 497, 563, doi: [10.1086/305479](https://doi.org/10.1086/305479)

Janiak, M., Sikora, M., & Moderski, R. 2016, *MNRAS*, 458, 2360, doi: [10.1093/mnras/stw465](https://doi.org/10.1093/mnras/stw465)

Levinson, A., & Rieger, F. 2011, *ApJ*, 730, 123, doi: [10.1088/0004-637X/730/2/123](https://doi.org/10.1088/0004-637X/730/2/123)

Lohfink, A. M., Reynolds, C. S., Jorstad, S. G., et al. 2013, *ApJ*, 772, 83, doi: [10.1088/0004-637X/772/2/83](https://doi.org/10.1088/0004-637X/772/2/83)

Lowell, B., Jacquemin-Ide, J., Tchekhovskoy, A., & Duncan, A. 2024, *ApJ*, 960, 82, doi: [10.3847/1538-4357/ad09af](https://doi.org/10.3847/1538-4357/ad09af)

Lyutikov, M. 2012, arXiv e-prints, arXiv:1209.3785, doi: [10.48550/arXiv.1209.3785](https://doi.org/10.48550/arXiv.1209.3785)

Marscher, A. P., Jorstad, S. G., Gómez, J.-L., et al. 2002, *Nature*, 417, 625, doi: [10.1038/nature00772](https://doi.org/10.1038/nature00772)

Misner, C. W., Thorne, K. S., & Wheeler, J. A. 1973, *Gravitation* (San Francisco: W.H. Freeman and Co.)

Mościbrodzka, M., Gammie, C. F., Dolence, J. C., & Shiokawa, H. 2011, *ApJ*, 735, 9, doi: [10.1088/0004-637X/735/1/9](https://doi.org/10.1088/0004-637X/735/1/9)

Narayan, R., & McClintock, J. E. 2012, *MNRAS*, 419, L69, doi: [10.1111/j.1745-3933.2011.01181.x](https://doi.org/10.1111/j.1745-3933.2011.01181.x)

Nathanail, A., & Contopoulos, I. 2014, *ApJ*, 788, 186, doi: [10.1088/0004-637X/788/2/186](https://doi.org/10.1088/0004-637X/788/2/186)

Nokhrina, E. E., Beskin, V. S., Kovalev, Y. Y., & Zheltoukhov, A. A. 2015, *MNRAS*, 447, 2726, doi: [10.1093/mnras/stu2587](https://doi.org/10.1093/mnras/stu2587)

O’ Riordan, M., Pe’er, A., & McKinney, J. C. 2018, *ApJ*, 853, 44, doi: [10.3847/1538-4357/aaa0c4](https://doi.org/10.3847/1538-4357/aaa0c4)

Page, D. N., & Thorne, K. S. 1974, *ApJ*, 191, 499, doi: [10.1086/152990](https://doi.org/10.1086/152990)

Parfrey, K., Philippov, A., & Cerutti, B. 2019, *PhRvL*, 122, 035101, doi: [10.1103/PhysRevLett.122.035101](https://doi.org/10.1103/PhysRevLett.122.035101)

Pjanka, P., Zdziarski, A. A., & Sikora, M. 2017, *MNRAS*, 465, 3506. <https://arxiv.org/abs/1607.08895>

Semenov, V., Dyadechkin, S., & Punsly, B. 2004, *Science*, 305, 978, doi: [10.1126/science.1100638](https://doi.org/10.1126/science.1100638)

Sikora, M., Nalewajko, K., & Madejski, G. M. 2020, *MNRAS*, 499, 3749, doi: [10.1093/mnras/staa3128](https://doi.org/10.1093/mnras/staa3128)

Sikora, M., Stawarz, L., & Lasota, J.-P. 2007, *ApJ*, 658, 815, doi: [10.1086/511972](https://doi.org/10.1086/511972)

Sitarz, M. C., Medvedev, M. V., & Ford, A. L. 2024, *ApJ*, 960, 4, doi: [10.3847/1538-4357/ad07d5](https://doi.org/10.3847/1538-4357/ad07d5)

Steiner, J. F., McClintock, J. E., & Narayan, R. 2013, *ApJ*, 762, 104, doi: [10.1088/0004-637X/762/2/104](https://doi.org/10.1088/0004-637X/762/2/104)

Tchekhovskoy, A., McKinney, J. C., & Narayan, R. 2012, in *Journal of Physics Conference Series*, Vol. 372, *Journal of Physics Conference Series* (IOP), 012040, doi: [10.1088/1742-6596/372/1/012040](https://doi.org/10.1088/1742-6596/372/1/012040)

Tchekhovskoy, A., Narayan, R., & McKinney, J. C. 2011, *MNRAS*, 418, L79, doi: [10.1111/j.1745-3933.2011.01147.x](https://doi.org/10.1111/j.1745-3933.2011.01147.x)

Thorne, K. S., Price, R. H., & MacDonald, D. A. 1986, *Black holes: The membrane paradigm* (Yale University Press)

Wald, R. M. 1974, *PhRvD*, 10, 1680, doi: [10.1103/PhysRevD.10.1680](https://doi.org/10.1103/PhysRevD.10.1680)

Woźniak, P. R., Zdziarski, A. A., Smith, D., Madejski, G. M., & Johnson, W. N. 1998, *MNRAS*, 299, 449, doi: [10.1046/j.1365-8711.1998.01831.x](https://doi.org/10.1046/j.1365-8711.1998.01831.x)

Yuan, Y., Chen, A. Y., & Luepker, M. 2025, *ApJ*, 985, 159, doi: [10.3847/1538-4357/adce79](https://doi.org/10.3847/1538-4357/adce79)

Zdziarski, A. A., & Egron, E. 2022, *ApJL*, 935, L4, doi: [10.3847/2041-8213/ac81bf](https://doi.org/10.3847/2041-8213/ac81bf)

Zdziarski, A. A., & Grandi, P. 2001, *ApJ*, 551, 186, doi: [10.1086/320064](https://doi.org/10.1086/320064)

Zdziarski, A. A., Phuravhathu, D. G., Sikora, M., Böttcher, M., & Chibueze, J. O. 2022a, *ApJL*, 928, L9, doi: [10.3847/2041-8213/ac5b70](https://doi.org/10.3847/2041-8213/ac5b70)

Zdziarski, A. A., Tetarenko, A. J., & Sikora, M. 2022b, *ApJ*, 925, 189, doi: [10.3847/1538-4357/ac38a9](https://doi.org/10.3847/1538-4357/ac38a9)